Published in final edited form as:
*Prog Neuropsychopharmacol Biol Psychiatry*. 2010 February 1; 34(1): 37. doi:10.1016/j.pnpbp.2009.09.015.

# The Kynurenine Pathway in Adolescent Depression: Preliminary Findings from a Proton MR Spectroscopy Study

**Vilma Gabbay, M.D., M.S.**[1,2], **Leonard Liebes, Ph.D**[3], **Yisrael Katz, B.S.**[1], **Songtao Liu, M.D.**[4], **Sandra Mendoza, B.S, M.A**[3], **James S. Babb, Ph.D.**[4], **Rachel G. Klein, Ph.D.**[1], and **Oded Gonen, Ph.D.**[4]

[1] NYU Child Study Center, Child and Adolescent Psychiatry, New York University School of Medicine, New York, New York. 577 First Avenue, New York, NY, 10016, United States

[2] Nathan S. Kline Institute, Orangeburg, NY. 140 Old Orangeburg Road, Orangeburg, NY, 10962, United States

[3] Cancer Institute, New York University School of Medicine, Tisch Hospital, 550 First Avenue, New York, NY, 10016, United States

[4] Radiology, Research, New York University School of Medicine, Bellevue C&D Building 122, 462 First Avenue, New York, NY, 10016, United States

## Abstract

**Background—**Cytokine induction of the enzyme indoleamine 2,3-dioxygenase (IDO) has been implicated in the development of major depressive disorder (MDD). IDO metabolizes tryptophan (TRP) into kynurenine (KYN), thereby decreasing TRP availability to the brain. KYN is further metabolized into several neurotoxins. The aims of this pilot were to examine possible relationships between plasma TRP, KYN, and 3-hydroxyanthranilic acid (3-HAA, neurotoxic metabolite) and striatal total choline (tCho, cell membrane turnover biomarker) in adolescents with MDD. We hypothesized that MDD adolescents would exhibit: i) positive correlations between KYN and 3-HAA and striatal tCho and a negative correlation between TRP and striatal tCho; and, ii) the anticipated correlations would be more pronounced in the melancholic subtype group.

**Methods—**Fourteen adolescents with MDD (seven with melancholic features) and six healthy controls were enrolled. Minimums of 6 weeks MDD duration and a severity score of 40 on the Children's Depression Rating Scale-Revised were required. All were scanned at 3 Tesla with MRI, multi-voxel 3-dimensional, high, 0.75 $cm^3$, spatial resolution proton magnetic resonance spectroscopic imaging. Striatal tCho concentrations were assessed using phantom replacement. Spearman correlation coefficients were Bonferroni-corrected.

**Results—**Positive correlations were found only in the melancholic group, between KYN and 3-HAA and tCho in the right caudate (r=0.93, $p$=0.03) and the left putamen (r=0.96, $p$=.006), respectively.

**Conclusions—**These preliminary findings suggest a possible role of the KYN pathway in adolescent melancholic MDD. Larger studies should follow.

### Keywords

Adolescent MDD; choline; kynurenine pathway; melancholic; MR Spectroscopy; striatum

## INTRODUCTION

Research of adolescent major depressive disorder (MDD) is highly important in light of the disorder's significant morbidity, and most critically, risk of suicide. Moreover, focusing on early-onset MDD may minimize the confounding effects of chronicity, treatment, and aging. At the same time, there is consensus that adolescent MDD is a heterogeneous clinical syndrome that reflects multiple etiologies. Yet, research identifying biological correlates of clinical subtypes of adolescent MDD has been scarce.

Mounting evidence has linked immune system activation with MDD. Clinical studies have documented increased pro-inflammatory cytokine plasma levels in adult and pediatric MDD (Gabbay et al., 2009; Irwin and Miller, 2007). One possible pathway linking cytokines with MDD involves the induction of the enzyme indoleamine 2,3-dioxygenase (IDO) by pro-inflammatory cytokines, particularly interferon-γ. IDO is the rate-limiting enzyme of the kynurenine pathway (KP) which metabolizes tryptophan (TRP) into kynurenine (KYN), thereby shunting TRP from the synthesis of serotonin. KYN is further metabolized into several neurotoxins, including 3-hydroxykynurenine (3-HK), 3-hydroxyanthranilic acid (3-HAA), and quinolinic acid (QUIN) (Goldstein et al., 2000; Schwarcz et al., 1983). In a competing branch of the KP, KYN is metabolized into kynurenic acid (KA), which blocks the neurotoxic effects of QUIN (Sapko et al., 2006). Activation of the KP has been hypothesized to contribute to glial loss and neuronal atrophy in specific brain regions in MDD (Myint et al., 2007; Wichers et al., 2005). This concept is supported by findings of enhanced KP activity and increased neurotoxic metabolite load in the plasma of adults with MDD compared to controls and in adults undergoing immunotherapy who developed depressive symptoms (Capuron et al., 2003; Myint et al., 2007; Wichers et al., 2005). While no studies have examined the KP in specific MDD subtypes, several investigations have reported lower values of plasma TRP/competing amino acids in adults with melancholic MDD compared to non-melancholic MDD and controls (Anderson et al., 1990; Maes et al., 1994; Maes et al., 1996), suggesting a role of the KP in melancholic MDD. However, findings based on plasma metabolite levels cannot be readily extrapolated to the central nervous system (CNS).

The use of proton magnetic resonance spectroscopic imaging ($^{1}$H MRSI) has the major advantage of affording *in vivo* non-invasive assessment of specific brain metabolites. Of relevance to MDD research is the brain metabolite total choline (tCho), which is associated with membrane phospholipid turnover, myelin breakdown, or changes in glial density, which have been documented in MDD (Hercher et al., 2009). As such, tCho alterations may result from KP metabolite neurotoxicity (See Fig. 1 for illustration of the KP and its relationship with tCho in MDD). Total Cho alterations have been repeatedly documented in adult and pediatric MDD (See Yildiz-Yesiloglu and Ankerst, 2006 for meta-analysis of $^{1}$H MRS studies in MDD). Studies of tCho in pediatric MDD have yielded diverse findings in different brain regions (Caetano, et al., 2005; Farchione, et al., 2002; Kusumakar, et al., 2001; Steingard et al., 2000). Focusing on the striatum, most studies in adult MDD have found increased tCho (Charles, et al., 1994; Hamakawa, et al., 1998; Vythilingam, et al., 2003), with only one study in adults yielding opposite results of decreased tCho/tCr (Renshaw, et al., 1997). Our group also documented increased tCho in the left caudate in adolescents with MDD (Gabbay et al., 2007). Other metabolites include the putative neuronal viability marker, N-acetyl-aspartate (NAA), and the cell bioenergetics component, total creatine (tCr). NAA and tCr alterations have not been consistently documented in most studies in MDD (Yildiz-Yesiloglu and Ankerst, 2006).

In this pilot, we aimed to examine relationships between plasma TRP, KYN, and 3-HAA concentrations and striatal tCho, NAA, and tCr in adolescents with MDD and controls with a focus on melancholic adolescent MDD. We examined the striatum (caudate and putamen) in

light of the large body of evidence implicating these structures in pediatric and adult MDD (Baumann et al., 1999; Forbes et al., 2009; Gabbay et al., 2007; Kim et al., 2008; Lacerda et al., 2003; Matsuo et al., 2008; Tremblay et al., 2005). Based on the above, hypotheses were that: i) only adolescents with MDD would exhibit positive correlations between KYN and 3-HAA and striatal tCho, and a negative correlation between TRP and striatal tCho, and; ii) the anticipated correlations would be more pronounced in the melancholic subtype group. No hypotheses were made regarding NAA and tCr since these metabolites have not been implicated in most $^{1}$H MRS studies of MDD.

## MATERIALS AND METHODS

### I. Subjects

The study was approved by the New York University (NYU) Institutional Review Board and the New York City Health and Hospital Corporation. Subjects described here were part of a previous $^{1}$H MRSI study (Gabbay et al., 2007).

**MDD Group—**Fourteen adolescents with MDD (eight female, 57%), ages 13–19 (16.5±2.0) were enrolled. All MDD subjects had to have a minimum duration of 6 weeks of a depressive episode and a minimum severity score of 40 on the Children's Depression Rating Scale – Revised (CDRS-R).

**Melancholic MDD—**The DSM-IV requires either severe anhedonia or lack of mood reactivity (Criteria A), and at least three of the following: distinct quality of depressed mood, marked psychomotor retardation or agitation, excessive guilt, mood worsening in the morning, and neurovegetative symptoms including sleep and appetite disturbances (Criteria B). We used a conservative diagnostic approach for melancholic MDD and required the presence of anhedonia and lack of mood reactivity along with at least 3 symptoms from Criteria B. By our study criteria, seven of the MDD subjects (three females, 43%), ages 13–19 (16.2±2.1) had melancholic features.

**Non-Melancholic MDD—**Seven adolescents with MDD (5 female, 71%), ages 13–19 (16.9 ±1.9) had non-melancholic, reactive MDD.

Adolescents with MDD were enrolled from the NYU Child Study Center, the NYU Tisch inpatient psychiatric unit, and the Bellevue Department of Psychiatry.

**Healthy Controls—**Six healthy comparison subjects (four female, 67%), ages 12–19 (16.2 ±2.4), recruited from families of NYU staff.

Participants age 18 and 19 ($n$ =4) provided signed informed consent; those under age 18 provided assent, and a parent signed consent. Adolescents (patients and controls) and a parent were interviewed by a child and adolescent psychiatrist using the Schedule for Affective Disorders and Schizophrenia-Present and Lifetime Version for Children (K-SADS-PL) (Kaufman et al., 1997), a semi-structured psychiatric interview. Based on the interview, the psychiatrist rated severity of depression on the CDRS-R, and overall adjustment on the Children's Global Assessment Scale (C-GAS). Participants completed the Beck Depression Inventory, 2$^{nd}$ ed. (BDI-II) and the Beck Scale for Suicidal Ideation (BSS).

Baseline medical assessments included medical history and laboratory tests, including complete blood count, metabolic panel, liver and thyroid function tests, urine toxicology test, and urine pregnancy test for females.

Exclusion criteria for all subjects included: immune-affecting medications taken in the past six months, any immunological or hematological disorder, chronic fatigue syndrome, any infection in the month prior to enrollment (including the common cold), significant medical or neurological disorders, a positive urine toxicology test, and in females, a positive urine pregnancy test.

The following lifetime psychiatric disorders were exclusionary for subjects with MDD: i) bipolar disorder, ii) schizophrenia, iii) pervasive developmental disorder, iv) post-traumatic stress disorder, v) obsessive-compulsive disorder, vi) Tourette's disorder, vii) eating disorder, and viii) a substance-related disorder in the past 12 months. Control subjects could not meet criteria for any major current or past DSM-IV diagnosis, and could not be taking psychotropic medications.

## II. Determination of Kynurenine Pathway Metabolite Concentrations

All blood samples (10 ml) were drawn between 08:00–09:00AM after an overnight fast (≥12h), processed within 20 minutes of collection, and stored at −80°C. All analyses were conducted by SM and LL, who were blind to the clinical status of subjects.

Calibration curves were prepared from stock solutions (100μg/ml) to yield the respective levels of TRP (1, 2, 4, 8, 12, and 14 μg/ml); KYN (0.05, 0.1, 0.2, 0.4, 1, 2, 4, and 5 μg/ml); and 3-HAA (0.1, 0.2, 0.4, 0.8, 2, and 3 μg/ml) in double distilled grade water and human plasma. The internal standard (3-nitro-L-tyrosine, 1 mg/ml) was also added to all calibration standards for recovery purposes.

Plasma (0.20 ml) was combined with 5 μl of 1 μg/μl 3-nitro-L-tyrosine followed by the addition of 0.20 ml of 0.05M $KH_2PO_4$ (pH 6.2). Subsequently, 50 μl of cold 2 M trichloroacetic acid were added, followed by vigorous vortexing. The mixture was centrifuged at 9,500 rpm for 10 minutes, and the supernatant was transferred into autosampler vials for analysis by high-performance liquid chromatography (HPLC). Aliquots of 200 μl of the supernatant were injected into the chromatographic system using a WISP model 717 autosampler (Waters Associates, Milford MA).

The eluted components of interest were detected as follows: (i) KYN and 3-nitro-L-tyrosine by tandem monitoring with UV absorption at 360 nm; (ii) TRP and 3-HAA by fluorescence monitoring at 340 nm (with UV excitation at 285 nm). A gradient elution was used for development of the chromatography in the following manner: The gradient consisted of a combination of two buffers: A (40 mM citrate buffer/0.1 mM succinic acid, disodium salt/0.05% sodium azide), and B (60% methanol/40 mM citrate buffer/0.1 mM succinic acid, disodium salt/0.05% sodium azide). The following sequence of steps was employed: 0–3 min, 0% B; 3–12 min, 0% B to 65%B (linear gradient); 12–18 min, 65% B; 18–20 min, 65% B to 100% B; 20–24 min 100% B; 24–26 min, 100% B to 0% B (linear gradient); 26–30 min 0% B. A flow rate of 0.8 ml/min was used during the 30 minute elution sequence of the analytical HPLC C18 column (4.6 × 150-mm, 5μm, Luna C18, Phenomenex, Torrance, CA).

## III. MR Data Acquisition

All experiments were done in a 3 Tesla (T) whole-body Magnetic Resonance Imaging (MRI) scanner (Trio, Siemens AG, Erlangen, Germany) using a TEM3000 transmit-receive head coil (MRI Instruments, Minneapolis, MN). For image-guidance of the MRS volume-of-interest (VOI), we used a sagittal 3D Magnetization Prepared RApid Gradient Echo (MP-RAGE): TE/TR/TI=2.7/2000/800 ms; and axial $T_2$-weighted: TE/TR=93/9090 ms, MRI. Both contrasts were acquired with 240×240 $mm^2$ field-of-view (FOV), but at 512×512 matrices and 3 mm thick slices for the $T_2$ and 256×256 matrices and 0.9 mm thick slices for the MP-RAGE.

A 10 cm anterior-posterior (AP) x7 cm left-right (LR) x6 cm inferior-superior (IS)=420 $cm^3$ VOI was image-guided onto the anatomy of interest, as shown in Fig. 2 and our chemical-shift imaging (CSI) based automatic shim procedure yielded consistent 23±3 Hz water linewidth from that volume (Hu et al., 1995). The VOI was excited using point-resolved spectroscopy (PRESS) *TE/TR*=135/1600 ms. Its selective 90° pulse interleaved two fourth-order Hadamard-encoded axial slabs (8 slices) per *TR* for optimal signal-to-noise-ratio (SNR) and duty-cycle (Goelman et al., 2006). This also enabled the use of 4 mT/m, gradients along the IS direction to limit chemical shift displacement between N-acetylaspartate (NAA) and tCho to 1 mm, *i.e.*, just ~15% of the slices' width (Goelman et al., 2007). The eight slices were 16×16 CSI encoded over 16×16 $cm^2$ FOV yielding 0.75 $cm^3$ voxels. The VOI was defined in the slices' LRxAP planes by two 12.8 ms long 180° numerically-optimized radio-frequency pulses. Under 1.0 (AP) and 1.2 mT/m (LR) gradients they sustained ~0.3 cm (30%) chemical shift displacement (but only at the VOI edges). The signals were acquired for 512 ms at ±1 KHz bandwidth. The MRS took 27 minutes and the entire protocol was completed in less than one hour.

**MRS Post Processing and quantification—**The MRS data were processed offline using in-house software. Residual water was removed from the free induction decays in the time domain. The data voxel-shifted to align the CSI grid with the NAA VOI, zero-filled from 16×16×8 to 256×256×8, apodized with a 3 Hz Lorentzian, Fourier transformed in the temporal, LR and AP direction and Hadamard reconstructed along the IS orientation. Although zero-filling does not add any *new* information content to the raw data, our rationale for choosing this strategy is that it can increase both the voxel signal-to-noise-ratio by approximately 40% (Ebel et al. 2006) as well as the effective spatial resolution by providing overlapping voxels. This *(i)* reduces partial volume artifacts at structures' edges (Du et al. 1994; Bernstein et al. 2001); and *(ii)* removes the need for several voxel shifts in order to optimize the position of the localization grip over each one of the four structures (left and right caudate and putamen) shown in Fig. 2 (Parker et al. 1995). No spatial filters were applied. The spectra were then automatically corrected for frequency and zero order phase shifts in reference to the NAA peak in each voxel (Goelman et al., 2006).

Relative levels of the $i^{th}$ ($i$=NAA, tCr, or tCho) metabolite in the $j^{th}$ subject were estimated from their peak area, $S_{ij}$, using spectral modeling software package SITools-FITT of Soher *et al.*, as shown in Fig. 2 (Soher et al., 1998). The $S_{ij}$ were then scaled into absolute concentrations, $C_{ij}$, relative to signals from a 2 L sphere of $C_i^{vitro}$=12.5, 10.0, 3.0 mM NAA, tCr, tCho water:

$$C_{ij} = C_i^{vitro} \cdot \frac{S_{ij}}{S_R} \cdot \frac{V_j^{180^\circ}}{V_R^{180^\circ}}, \quad [1]$$

where $S_R$ is the sphere's metabolite signal, $V_j^{180^\circ}$, and $V_R{}^{180\circ}$ are the RF voltages needed for a non-selective 1 ms 180° inversion pulse on subject and reference sphere. The $C_{ij}$s were corrected for relaxation time differences *in vivo* ($T_1^{vivo}$, $T_2^{vivo}$) and in the phantom ($T_1^{vitro}$, $T_2^{vitro}$) with a scaling factor (Inglese et al., 2003):

$$f = \frac{\exp\left(-TE/T_2^{vitro}\right)}{\exp\left(-TE/T_2^{vivo}\right)} \cdot \frac{1 - \exp\left(TR/T_1^{vitro}\right)}{1 - \exp\left(TR/T_1^{vivo}\right)} \quad (2)$$

using the $T_1^{vivo}$ =1.4, 1.3 and 1.2 s, $T_2^{vivo}$= 343, 172 and 248 ms reported at 3 T for NAA, tCr and tCho (Kirov et al., 2008;Traber et al., 2004) and $T_1^{vitro}$=605, 336 and 235 ms, $T_2^{vitro}$=483, 288 and 200 ms measured in the phantom.

For each subject the $^1$H MRS slice that contained the largest cross-section of the striatum was selected based on the axial MRI, as shown in Fig. 2. The caudate and the putamen were then manually circumscribed (in each subject) and our software summed the spectra in all the voxels that fell completely or partially within the outline (see Fig. 2). The software then calculated: i) the circumscribed region's volume, (i.e. the sum of all the circumscribed voxels); ii) the average of the relative concentrations, $C_{ij}$, for each of the three metabolites; and iii) their standard deviations (SD).

### IV. Statistical Analysis

Spearman rank correlation coefficients were used to characterize the association of KP metabolite plasma levels with tCho, NAA, and tCr striatal concentrations for all subjects. Bonferroni corrections within domain were applied (x12). An Exact Mann-Whitney test was used to compare KP metabolites and striatal tCho between medicated and non-medicated MDD adolescents. All reported *p*-values are two-sided significance levels with the appropriate Bonferroni correction. Statistical significance was defined as $p \leq 0.05$. SAS version 9.0 (SAS Institute, Cary, NC) was used for all statistical computations.

## RESULTS

### I. Participants

Demographics, diagnoses, and treatment profiles are compiled in Table 1.

**MDD group—**Of the fourteen subjects with MDD, nine subjects were treated with psychotropic medications for periods ranging from one month to two-and-a-half years. All patients on medication had failed to respond to treatment at the time of the blood draw and scan. Medications included fluoxetine, sertraline, bupropion, lamotrigine, lithium, risperidone, and quetiapine.

### II. Volumetry

The volumes of circumscribed ROIs (mean±SD) were as follows: **MDD subjects:** caudate: 811±59 left (L) and 796±49 mm$^3$ right (R), putamen: 885±84 (L) and 903±84 mm$^3$ (R). **Controls:** caudate: 821±38 (L) versus 796±31 mm$^3$ (R), putamen: 889±77 (L) versus 880±74 mm$^3$ (R). Neither region showed any significant difference between sides (left versus right) or groups (patients versus controls) ($p>0.1$). It is noteworthy that these ROIs included edge-voxels even when they only partly fell within the circumscribed region. To estimate the edge-voxels partial volume contribution we considered their surface-to-volume ratio. With an MRI pixel volume of 2.9 mm$^3$ and striatum (caudate and putamen) ROI volumes of ~1600 mm$^3$, ~30 out of 550 voxels were at the surface, where their partial volume can range anywhere from 1 to 99%. Assuming an average partial volume of 50% in these edge-voxels, however, renders the partial volume to be ~8%. Since this (small) fraction was very similar amongst all the patients and the controls, it was deemed negligible for the purpose of this comparative analysis.

### III. Associations between Plasma Kynurenines and Striatal tCho, NAA, tCr Concentrations

Patients' and controls' TRP, KYN, and 3-HAA plasma concentrations as well as tCho NAA, and tCr concentrations from the left and right caudate and putamen are compiled in Table 2.

No significant correlations were found in the healthy control group or in the MDD group as a whole. When each MDD subgroup was examined separately, positive correlations were found

only in the melancholic subgroup: i) plasma KYN concentrations were positively correlated with right caudate tCho (r=0.93, *p*=0.03, Bonferroni corrected x12, Fig. 3a,c); ii) plasma 3-HAA, a neurotoxic intermediate of the KP, was positively correlated with left putamen tCho (r=0.96, *p*=.006, Bonferroni corrected x12, Fig. 3b,d).

There were no significant differences between adolescents with MDD who were treated with psychotropic medications (*n*=9) and who were medication naïve/free (*n*=5) with respect to striatal tCho and KP metabolites.

There were also no significant correlations between striatal NAA and tCr with TRP, KYN, and 3-HAA in any of the examined groups.

## DISCUSSION

This is the first study that examines the possible relationship between KP metabolites and brain chemistry using $^{1}$H MRSI. We found two positive correlations only in the subgroup of melancholic adolescent MDD: i) KYN plasma concentrations and tCho in the right caudate, and ii) 3-HAA plasma concentrations and tCho in the left putamen. Our findings suggest that the neurobiology of melancholic adolescent MDD is distinct from other subtypes of depression and that a possible relationship may exist between KP metabolites and striatal tCho in that subgroup of patients.

Choline is an essential component of membrane lipids, phosphatidylcholine, and sphingomyelin (Loffelholz et al., 1993). The resonance of tCho at 3.22 ppm comprises mostly the quaternary *N*-methyl groups of the cytosolic compounds glycerolphosphocholine (breakdown products) and phosphocholine (membrane precursors). The contribution of free Cho to the signal is less than 5% and acetylcholine's is negligible (Miller et al., 1996). Total Cho has been hypothesized to reflect cell membrane metabolism (both breakdown and proliferation), myelin breakdown, or changes in glial density (Urenjak et al., 1993), which have been documented in the frontal cortex and sub-cortical regions in MDD (Hercher et al., 2009). Therefore, our findings of positive correlations between KYN and 3-HAA and striatal tCho suggest that pathways involved in cellular survival may be more relevant to the pathogenesis of melancholic adolescent MDD compared to other subtypes of MDD. This notion is supported by findings from adult MDD studies documenting reductions of γ-aminobutyric acid (GABA) concentrations in the plasma (Petty et al., 1992), the CSF (Roy et al., 1991), and the occipital lobe (Sanacora et al., 2004) as well as increased glutamate brain concentrations (Sanacora et al., 2004), which were more pronounced in melancholic MDD patients compared to controls.

In relation to MDD, the neurotoxic effects of QUIN, a KP metabolite, are of specific interest. QUIN is an agonist of an NMDA glutamate receptor subtype which has been attributed a key role in MDD (Perkins and Stone, 1982). QUIN alone has been shown to increase glutamate and decrease GABA brain concentrations (Schwarcz et al., 1983; Tavares et al., 2002). As such, QUIN may contribute to the increased glutamate and decreased GABA concentrations observed in melancholic MDD. Three-HK and 3-HAA, other neurotoxins derived from the KP, are thought to induce oxidative stress. Animal studies indicate that 3-HK and 3-HAA toxicity has brain region selectivity with the striatum, our region of interest, being particularly vulnerable to these toxins (Okuda et al., 1998).

Our findings also suggest the possible neurotoxic effects of peripheral activation of the KP in adolescent melancholic MDD. This interpretation is supported by a recent animal study documenting that peripheral administration of KYN alone induced depressive-like symptoms, and that systemic inhibition of IDO activity blocked the development of depressive-like

symptoms in mice (i.e. duration of immobility in forced-swim and tail suspension tests) following an immunological challenge with lipopolysaccharide (O'Connor et al., 2009).

Our findings implicating the KP in melancholic adolescent MDD are consistent with several observations in adults documenting lower values of plasma TRP/competing amino acids in melancholic adult MDD subjects compared to non-melancholic MDD subjects and controls (Anderson et al., 1990; Maes et al., 1994; Maes et al., 1996). In an early study from 1970, Curzon and Bridges found that females with "endogenous" depression (i.e. melancholic MDD) exhibited increased excretion of KYN and 3-HK in urine compared to controls after an oral load of TRP (Curzon and Bridges, 1970). Additionally, findings of highest plasma levels of neopterin, a pteridine released from macrophages/monocytes in parallel to IDO activity, in the melancholic MDD group also provide support for the role of the KP in melancholic MDD (Maes et al., 1994). More recently, Capuron et al. documented a positive correlation between the development of neurovegetative symptoms, prominent features of melancholic MDD, and the reduction of plasma TRP in adult cancer patients who underwent treatment with IFN-α or IL-2 (Capuron et al., 2002).

Finally, our correlations involved both the left putamen and the right caudate and fit a large body of evidence implicating both of these structures in adult and pediatric MDD (Forbes et al., 2009; Gabbay et al., 2007; Matsuo et al., 2008).

Our findings should be considered preliminary in light of several limiting factors: one, the cohort size is modest and may have limited the identification of other relationships and contributed to Type II errors. However, multiple hypotheses corrections were applied to the analysis to minimize Type I errors. Also, most MDD patients were on medication at the time of the scan. All the MDD adolescents in our study were depressed at the time of their scan, and there were no metabolite differences between MDD adolescents who were treated with medications and those who were not.

In summary, our preliminary findings suggest a possible relationship between KP metabolites and striatal membrane-turnover in melancholic adolescent MDD and that pathways involved in cellular survival may be more relevant to the pathogenesis of melancholic adolescent MDD compared to other subtypes of MDD. Studies with larger sample size should follow. Possible relationships between the KP and other brain metabolites such as GABA and glutamate should be examined as well.

## Acknowledgments

This study was supported by grants from NIH (AT002395, AT004576, MH077072, NS050520 and EB01015), the American Foundation for Suicide Prevention, the NYU School of Medicine General Clinical Research Center grant (M01-RR00096), and generous gifts from the Leon Levy Foundation, the Anita Saltz Foundation, and from Bruce and Claude Wasserstein. The authors thank Dr. Andrew A. Maudsley of the University of Miami and Brian J. Soher of Duke University for the use of their SITools-FITT spectral modeling software package. The authors also thank F. Xavier Castellanos for his helpful comments on this manuscript.

## ABBREVIATIONS

| | |
|---|---|
| 3-HAA | 3-hydroxyanthranilic acid |
| 3-HK | 3-hydroxykynurenine |
| AP | anterior-posterior |
| BDI-II | Beck Depression Inventory, 2nd ed |
| BSS | Beck Scale for Suicidal Ideation |

| | |
|---|---|
| CDRS-R | Children's Depression Rating Scale – Revised |
| C-GAS | Children's Global Assessment Scale |
| CNS | central nervous system |
| CSI | chemical-shift imaging |
| FOV | field-of-interest |
| GABA | γ-aminobutyric acid |
| $^{1}$H MRSI | proton magnetic resonance spectroscopic imaging |
| IDO | indoleamine 2,3-dioxygenase |
| HPLC | high-performance liquid chromatography |
| IFN | interferon |
| IL | interleukin |
| IS | inferior-superior |
| KA | kynurenic acid |
| KP | kynurenine pathway |
| K-SADS-PL | Schedule for Affective Disorders and Schizophrenia-Present and Lifetime Version for Children |
| KYN | kynurenine |
| LR | left-right |
| MDD | major depressive disorder |
| MRI | Magnetic Resonance Imaging |
| NAA | N-acetylaspartate |
| NYU | New York University |
| PRESS | point-resolved spectroscopy |
| QUIN | quinolinic acid |
| ROI | region of interest |
| SNR | signal-to-noise-ratio |
| tCho | total choline |
| tCr | total creatine |
| TRP | tryptophan |
| VOI | volume of interest |

## References

Anderson IM, Parry-Billings M, Newsholme EA, Poortmans JR, Cowen PJ. Decreased plasma tryptophan concentration in major depression: relationship to melancholia and weight loss. J Affect Disord 1990;20:185–91. [PubMed: 2148339]

Baumann B, Danos P, Krell D, Diekmann S, Leschinger A, Stauch R, et al. Reduced volume of limbic system-affiliated basal ganglia in mood disorders: preliminary data from a postmortem study. J Neuropsychiatry Clin Neurosci 1999;11:71–8. [PubMed: 9990559]

Bernstein MA, Fain SB, Riederer SJ. Effect of windowing and zero-filled reconstruction of MRI data on spatial resolution and acquisition strategy. J Magn Reson Imaging 2001;14:270–80. [PubMed: 11536404]

Caetano SC, Fonseca M, Olvera RL, Nicoletti M, Hatch JP, Stanley JA, et al. Proton spectroscopy study of the left dorsolateral prefrontal cortex in pediatric depressed patients. Neurosci Lett 2005;384:321–6. [PubMed: 15936878]

Capuron L, Neurauter G, Musselman DL, Lawson DH, Nemeroff CB, Fuchs D, et al. Interferon-alpha-induced changes in tryptophan metabolism. relationship to depression and paroxetine treatment. Biol Psychiatry 2003;54:906–14. [PubMed: 14573318]

Capuron L, Ravaud A, Neveu PJ, Miller AH, Maes M, Dantzer R. Association between decreased serum tryptophan concentrations and depressive symptoms in cancer patients undergoing cytokine therapy. Mol Psychiatry 2002;7:468–73. [PubMed: 12082564]

Charles HC, Lazeyras F, Krishnan KR, Boyko OB, Payne M, Moore D. Brain choline in depression: in vivo detection of potential pharmacodynamic effects of antidepressant therapy using hydrogen localized spectroscopy. Prog Neuropsychopharmacol Biol Psychiatry 1994;18:1121–7. [PubMed: 7846284]

Curzon G, Bridges PK. Tryptophan metabolism in depression. J Neurol Neurosurg Psychiatry 1970;33:698–704. [PubMed: 5478953]

Du YP, Parker DL, Davis WL, Cao G. Reduction of partial-volume artifacts with zero-filled interpolation in three-dimensional MR angiography. J Magn Res Imaging 1994;4:733–741.

Ebel A, Dreher W, Leibfritz D. Effects of zero-filling and apodization on spectral integrals in discrete Fourier-transform spectroscopy of noisy data. J Magn Reson 2006;182:330–338. [PubMed: 16844391]

Farchione TR, Moore GJ, Rosenberg DR. Proton magnetic resonance spectroscopic imaging in pediatric major depression. Biol Psychiatry 2002;52:86–92. [PubMed: 12113999]

Forbes EE, Hariri AR, Martin SL, Silk JS, Moyles DL, Fisher PM, et al. Altered striatal activation predicting real-world positive affect in adolescent major depressive disorder. Am J Psychiatry 2009;166:64–73. [PubMed: 19047324]

Gabbay V, Hess DA, Liu S, Babb JS, Klein RG, Gonen O. Lateralized Caudate Metabolic Abnormalities in Adolescent Major Depressive Disorder: A Proton MR Spectroscopy Study. Am J Psychiatry 2007;164:1881–9. [PubMed: 18056244]

Gabbay V, Klein RG, Alonso CM, Babb JS, Nishawala M, De Jesus G, et al. Immune system dysregulation in adolescent major depressive disorder. J Affect Disord 2009;115:177–82. [PubMed: 18790541]

Goelman G, Liu S, Fleysher R, Fleysher L, Grossman RI, Gonen O. Chemical-shift artifact reduction in Hadamard-encoded MR spectroscopic imaging at high (3T and 7T) magnetic fields. Magn Reson Med 2007;58:167–73. [PubMed: 17659608]

Goelman G, Liu S, Hess D, Gonen O. Optimizing the efficiency of high-field multivoxel spectroscopic imaging by multiplexing in space and time. Magn Reson Med 2006;56:34–40. [PubMed: 16767711]

Goldstein LE, Leopold MC, Huang X, Atwood CS, Saunders AJ, Hartshorn M, et al. 3-Hydroxykynurenine and 3-hydroxyanthranilic acid generate hydrogen peroxide and promote alpha-crystallin cross-linking by metal ion reduction. Biochemistry 2000;39:7266–75. [PubMed: 10852726]

Hamakawa H, Kato T, Murashita J, Kato N. Quantitative proton magnetic resonance spectroscopy of the basal ganglia in patients with affective disorders. Eur Arch Psychiatry Clin Neurosci 1998;248:53–8. [PubMed: 9561353]

Hercher C, Turecki G, Mechawar N. Through the looking glass: Examining neuroanatomical evidence for cellular alterations in major depression. J Psychiatr Res 2009;43:947–61. [PubMed: 19233384]

Hu J, Javaid T, Arias-Mendoza F, Liu Z, McNamara R, Brown TR. A fast, reliable, automatic shimming procedure using 1H chemical-shift-imaging spectroscopy. J Magn Reson B 1995;108:213–9. [PubMed: 7670755]

Inglese M, Li BS, Rusinek H, Babb JS, Grossman RI, Gonen O. Diffusely elevated cerebral choline and creatine in relapsing-remitting multiple sclerosis. Magn Reson Med 2003;50:190–5. [PubMed: 12815694]

Irwin MR, Miller AH. Depressive disorders and immunity: 20 years of progress and discovery. Brain Behav Immun 2007;21:374–83. [PubMed: 17360153]

Kaufman J, Birmaher B, Brent D, Rao U, Flynn C, Moreci P, et al. Schedule for Affective Disorders and Schizophrenia for School-Age Children-Present and Lifetime Version (K-SADS-PL): initial reliability and validity data. J Am Acad Child Adolesc Psych 1997;36:980–8.

Kim MJ, Hamilton JP, Gotlib IH. Reduced caudate gray matter volume in women with major depressive disorder. Psychiatry Res 2008;164:114–22. [PubMed: 18930633]

Kirov I, Fleysher L, Fleysher R, Patil V, Liu S, Gonen O. Age dependence of regional proton metabolites T2 relaxation times in the human brain at 3 T. Magn Reson Med 2008;60:790–5. [PubMed: 18816831]

Kusumakar V, MacMaster FP, Gates L, Sparkes SJ, Khan SC. Left medial temporal cytosolic choline in early onset depression. Can J Psychiatry 2001;46:959–64. [PubMed: 11816318]

Lacerda AL, Nicoletti MA, Brambilla P, Sassi RB, Mallinger AG, Frank E, et al. Anatomical MRI study of basal ganglia in major depressive disorder. Psychiatry Res 2003;124:129–40. [PubMed: 14623065]

Loffelholz K, Klein J, Koppen A. Choline, a precursor of acetylcholine and phospholipids in the brain. Prog Brain Res 1993;98:197–200. [PubMed: 8248509]

Maes M, Scharpe S, Meltzer HY, Okayli G, Bosmans E, D'Hondt P, et al. Increased neopterin and interferon-gamma secretion and lower availability of L-tryptophan in major depression: further evidence for an immune response. Psychiatry Res 1994;54:143–60. [PubMed: 7761549]

Maes M, Wauters A, Verkerk R, Demedts P, Neels H, Van Gastel A, et al. Lower serum L-tryptophan availability in depression as a marker of a more generalized disorder in protein metabolism. Neuropsychopharmacology 1996;15:243–51. [PubMed: 8873107]

Matsuo K, Rosenberg DR, Easter PC, MacMaster FP, Chen HH, Nicoletti M, et al. Striatal volume abnormalities in treatment-naive patients diagnosed with pediatric major depressive disorder. J Child Adolesc Psychopharmacol 2008;18:121–31. [PubMed: 18439110]

Miller DH, Albert PS, Barkhof F, Francis G, Frank JA, Hodgkinson S, et al. Guidelines for the use of magnetic resonance techniques in monitoring the treatment of multiple sclerosis. US National MS Society Task Force. Ann Neurol 1996;39:6–16. [PubMed: 8572668]

Myint AM, Kim YK, Verkerk R, Scharpe S, Steinbusch H, Leonard B. Kynurenine pathway in major depression: evidence of impaired neuroprotection. J Affect Disord 2007;98:143–51. [PubMed: 16952400]

O'Connor JC, Lawson MA, Andre C, Moreau M, Lestage J, Castanon N, et al. Lipopolysaccharide-induced depressive-like behavior is mediated by indoleamine 2,3-dioxygenase activation in mice. Mol Psychiatry 2009;14:511–22. [PubMed: 18195714]

Okuda S, Nishiyama N, Saito H, Katsuki H. 3-Hydroxykynurenine, an endogenous oxidative stress generator, causes neuronal cell death with apoptotic features and region selectivity. J Neurochem 1998;70:299–307. [PubMed: 9422375]

Parker DL, Du YP, Davis WL. The Voxel Sensitivity Function In Fourier Transform Imaging: Application to Magnetic Rersonance Angiography. Magn Reson Med 1995;32:156–160. [PubMed: 7707904]

Perkins MN, Stone TW. An iontophoretic investigation of the actions of convulsant kynurenines and their interaction with the endogenous excitant quinolinic acid. Brain Res 1982;247:184–7. [PubMed: 6215086]

Petty F, Kramer GL, Gullion CM, Rush AJ. Low plasma gamma-aminobutyric acid levels in male patients with depression. Biol Psychiatry 1992;32:354–63. [PubMed: 1420649]

Renshaw PF, Lafer B, Babb SM, Fava M, Stoll AL, Christensen JD, et al. Basal ganglia choline levels in depression and response to fluoxetine treatment: an in vivo proton magnetic resonance spectroscopy study. Biol Psychiatry 1997;41:837–43. [PubMed: 9099409]

Roy A, Dejong J, Ferraro T. CSF GABA in depressed patients and normal controls. Psychol Med 1991;21:613–8. [PubMed: 1719577]

Sanacora G, Gueorguieva R, Epperson CN, Wu YT, Appel M, Rothman DL, et al. Subtype-specific alterations of gamma-aminobutyric acid and glutamate in patients with major depression. Arch General Psychiatry 2004;61:705–13.

Sapko MT, Guidetti P, Yu P, Tagle DA, Pellicciari R, Schwarcz R. Endogenous kynurenate controls the vulnerability of striatal neurons to quinolinate: Implications for Huntington's disease. Exp Neurol 2006;197:31–40. [PubMed: 16099455]

Schwarcz R, Whetsell WO Jr, Mangano RM. Quinolinic acid: an endogenous metabolite that produces axon-sparing lesions in rat brain. Science 1983;219:316–8. [PubMed: 6849138]

Soher BJ, Young K, Govindaraju V, Maudsley AA. Automated spectral analysis III: application to in vivo proton MR spectroscopy and spectroscopic imaging. Magn Reson Med 1998;40:822–31. [PubMed: 9840826]

Steingard RJ, Yurgelun-Todd DA, Hennen J, Moore JC, Moore CM, Vakili K, et al. Increased orbitofrontal cortex levels of choline in depressed adolescents as detected by in vivo proton magnetic resonance spectroscopy. Biol Psychiatry 2000;48:1053–61. [PubMed: 11094138]

Tavares RG, Tasca CI, Santos CE, Alves LB, Porciuncula LO, Emanuelli T, et al. Quinolinic acid stimulates synaptosomal glutamate release and inhibits glutamate uptake into astrocytes. Neurochem Int 2002;40:621–7. [PubMed: 11900857]

Traber F, Block W, Lamerichs R, Gieseke J, Schild HH. 1H metabolite relaxation times at 3.0 tesla: Measurements of T1 and T2 values in normal brain and determination of regional differences in transverse relaxation. J Magn Reson Imaging 2004;19:537–45. [PubMed: 15112302]

Tremblay LK, Naranjo CA, Graham SJ, Herrmann N, Mayberg HS, Hevenor S, et al. Functional neuroanatomical substrates of altered reward processing in major depressive disorder revealed by a dopaminergic probe. Arch Gen Psychiatry 2005;62:1228–36. [PubMed: 16275810]

Urenjak J, Williams SR, Gadian DG, Noble M. Proton nuclear magnetic resonance spectroscopy unambiguously identifies different neural cell types. J Neurosci 1993;13:981–9. [PubMed: 8441018]

Vythilingam M, Charles HC, Tupler LA, Blitchington T, Kelly L, Krishnan KR. Focal and lateralized subcortical abnormalities in unipolar major depressive disorder: an automated multivoxel proton magnetic resonance spectroscopy study. Biol Psychiatry 2003;54:744–50. [PubMed: 14512215]

Wichers MC, Koek GH, Robaeys G, Verkerk R, Scharpe S, Maes M. IDO and interferon-alpha-induced depressive symptoms: a shift in hypothesis from tryptophan depletion to neurotoxicity. Mol Psychiatry 2005;10:538–44. [PubMed: 15494706]

Yildiz-Yesiloglu A, Ankerst DP. Review of 1H magnetic resonance spectroscopy findings in major depressive disorder: a meta-analysis. Psychiatry Res 2006;147:1–25. [PubMed: 16806850]

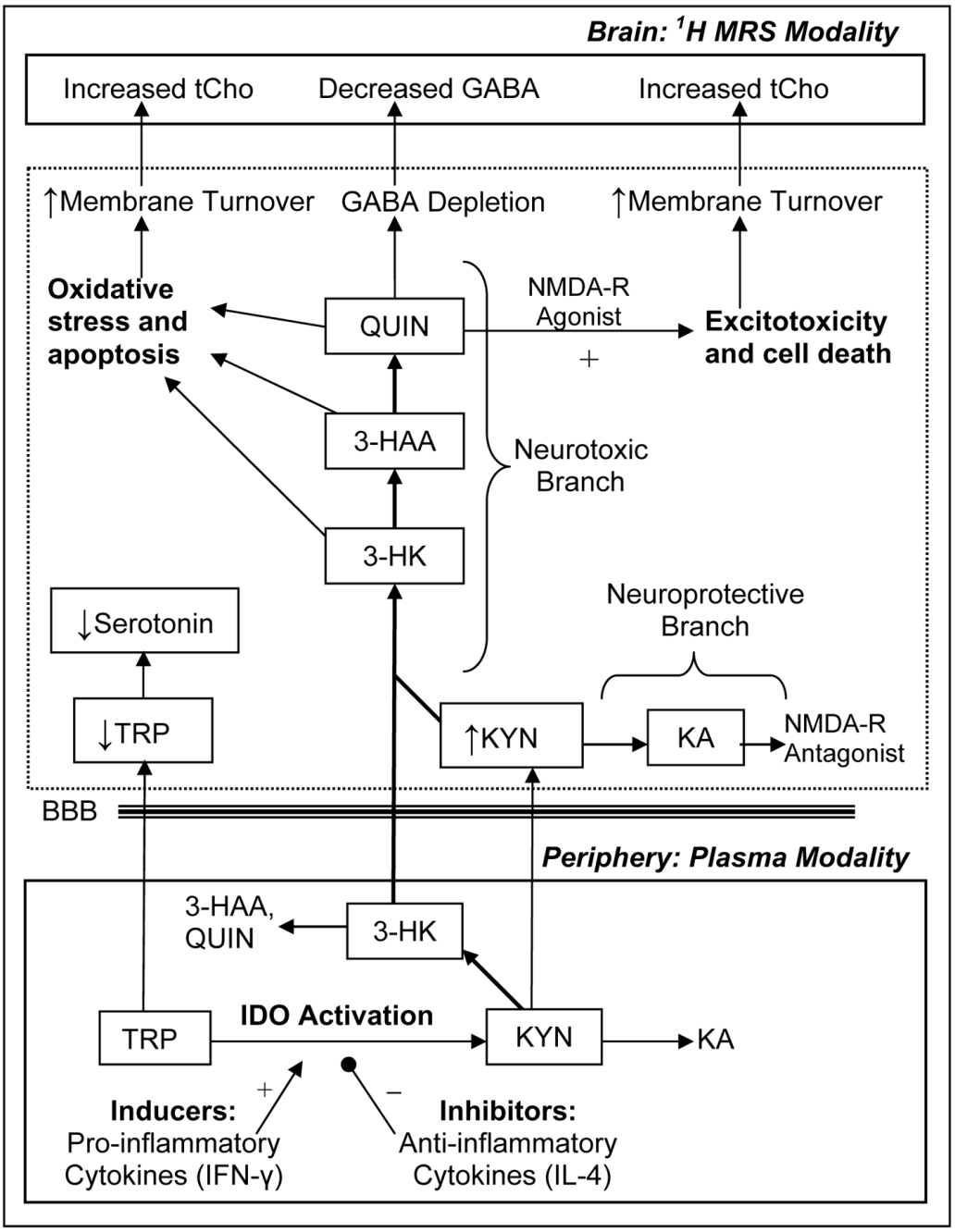


**Figure 1.**
Possible neurotoxic consequences of kynurenine pathway activation. TRP, tryptophan; IFN, interferon; IL, interleukin; 3-HK, 3-hydroxykynurenine; 3-HAA, 3-hydroxyanthranilic acid; QUIN, quinolinic acid; KA, kynurenic acid; BBB, blood-brain barrier; NMDA-R, N-methyl-D-aspartate receptor; tCho, Total Choline; GABA, γ-aminobutyric acid.

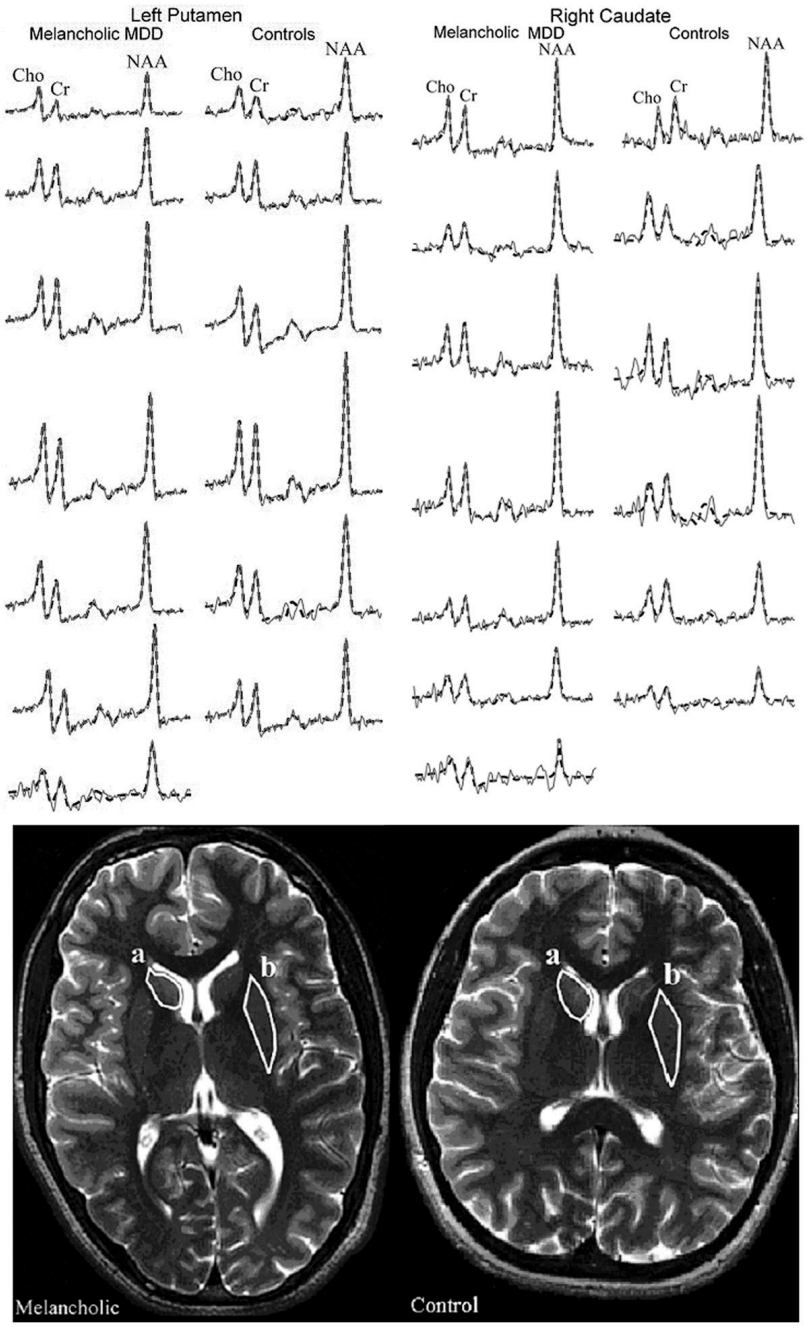


**Figure 2.**

**(Top)** Real part of the summed spectra (thin gray line) in the left putamen (circumscribed region b) and right caudate (circumscribed region a) overlaid with their SITools-FITT model functions (dashed black lines) from the 7 melancholic major depressive disorder (MDD) patients (left columns) and 6 healthy controls (right columns). All spectra are on common intensity and frequency scales. Note the regional signal-to-noise-ratios and quality of the fit procedure from which the values for metabolic quantifications with Eq. [1] were obtained. **(Bottom)** Axial *T2*-weighted images from an MDD adolescent with melancholic features (left) and a gender- and age-matched control (right), both superimposed with outlines (white line)

of the right caudate (a) and left putamen (b) that were used for volumetry and metabolic quantification.

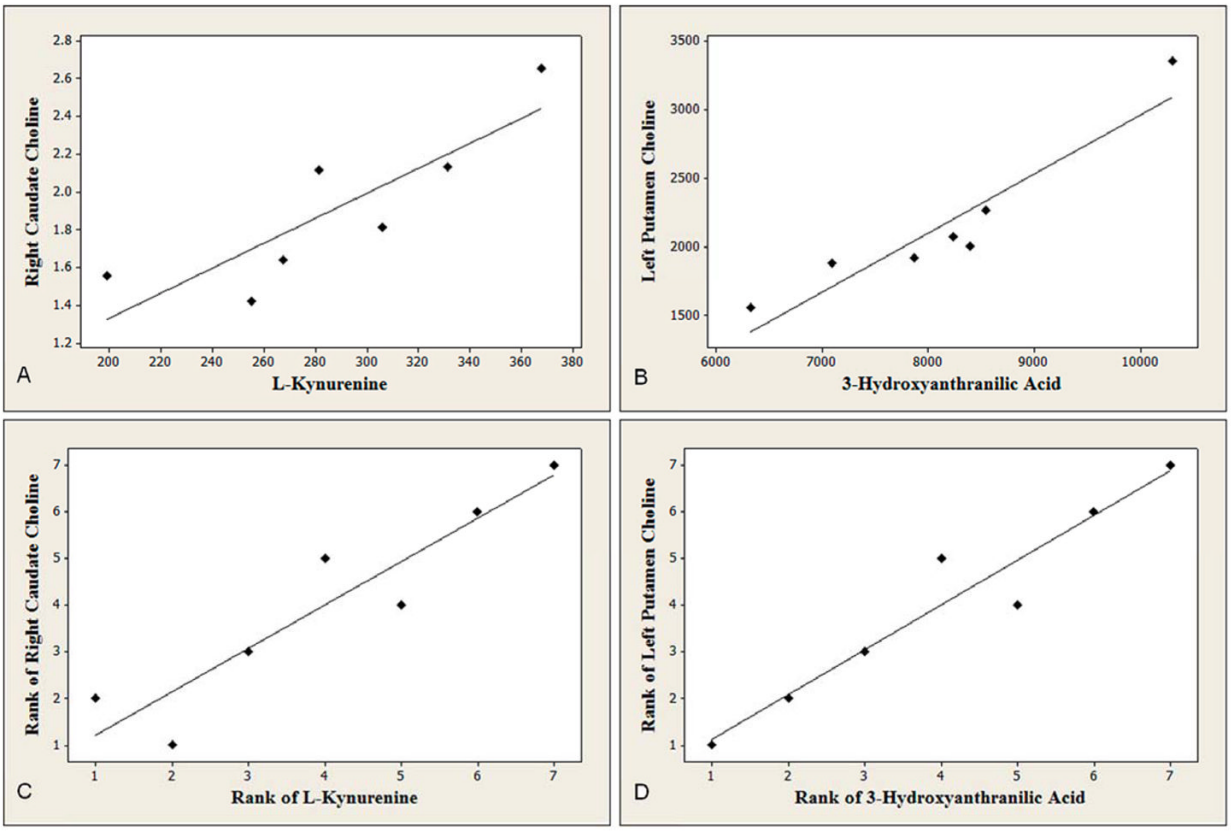


**Figure 3.**

Scatter plots with regression lines characterizing associations of L-kynurenine (KYN) metabolite plasma levels and striatal total choline (tCho), for the seven adolescents with major depressive disorder in the melancholic subgroup. **(A)** Plasma KYN concentrations (ng/ml) and tCho (mM) in the right caudate (Spearman correlation: r=0.93, $p$=0.03); **(B)** plasma 3-hydroxyantranilic acid (3-HAA) concentrations (ng/ml) and tCho (mM) in the left putamen (r=0.96, $p$=.006); **(C)** ranks of KYN and right caudate tCho; **(D)** ranks of 3-HAA and left putamen tCho. All reported $p$-values are Bonferroni-corrected within domain (x12) two-sided significance levels. Statistical significance was defined as $p \leq 0.05$.

## Table 1

Demographic and Clinical Characteristics of Major Depressive Disorder (MDD) Adolescents with Melancholic Features, MDD Adolescents without Melancholic Features, and Healthy Adolescent Controls

| Characteristic | MDD Adolescents with Melancholic Features *n*=7 | MDD Adolescents without Melancholic Features *n*=7 | Healthy Adolescent Controls *n*=6 |
|---|---|---|---|
| Age (years) | 16.2 ± 2.1 | 16.9 ± 1.9 | 16.2 ± 2.4 |
| Gender (male/female) | 4/3 [a](57/43%) | 2/5 [a](29/71%) | 2/4 [a](33/67%) |
| **Illness History** | | | |
| Duration of Illness (months) | 17.6 ± 9.2 [b](3–30) | 16.9 ± 14.2 [b](1.5–36) | 0 |
| Medication-naïve/Medication-free/Medicated | 2/1/4 [a](29/14/57%) | 2/0/5 [a](29/0/71%) | 6/0/0 [a](100/0/0%) |
| [c] CDRS-R | 74.9 ± 7.4 [b](60–83) | 51.7 ± 12.5 [b](40–75) | 18.2 ± 2.4 [b](17–23) |
| [d] BDI-II | 25.5 ± 12.6 [b](12–44) | 26.7 ± 15.3 [b](6–50) | 2.2 ± 1.9 [b](0–5) |
| [e] BSS | 12.6 ± 10.5 [b](1–24) | 7.3 ± 7.3 [b](0–20) | 0.0 ± 0.0 [b](0) |
| **Current Comorbidity** | | | |
| [f] ADHD | 1 [a](14.3%) | 1 [a](14.3%) | 0 |
| Social Phobia | 1 [a](14.3%) | 1 [a](14.3%) | 0 |
| Any Comorbidity | 2 [a](28.6%) | 2 [a](28.6%) | 0 |

[a] Respective percentages (may not add up to 100% due to rounding);

[b] Range;

[c] Children's Depression Rating Scale-Revised;

[d] Beck Depression Inventory-II;

[e] Beck Scale for Suicidal Ideation;

[f] Attention Deficit Hyperactivity Disorder.

**Table 2**

Tryptophan (TRP), Kynurenine (KYN), and 3-Hydroxyantranilic Acid (3-HAA) Plasma Concentrations (in ng/ml) and Total Choline (tCho), N-Acetylaspartate (NAA), and Total Creatine (tCr) Levels, Scaled into Concentrations (in mM) Using Phantom Replacement, in the Left and Right Caudate and Putamen of Adolescents with Major Depressive Disorder (MDD) with and without Melancholic Features, All MDD Adolescents, and Healthy Adolescent Controls.

| **Measure** | **MDD Adolescents with Melancholic Features *n*=7** | | **MDD Adolescents without Melancholic Features *n*=7** | | **All MDD Adolescents *n*=14** | | **Healthy Adolescent Controls *n*=6** | |
|---|---|---|---|---|---|---|---|---|
| **Plasma Concentration (ng/ml)** | **Mean** | **[g]SD** | **Mean** | **SD** | **Mean** | **SD** | **Mean** | **SD** |
| [a]3-HAA | 8106 | 1252 | 7350 | 2535 | 7757 | 1901 | 7464 | 1708 |
| [b] KYN | 287 | 55 | 296 | 97 | 291 | 74 | 267 | 68 |
| [c] TRP | 583 | 323 | 846 | 469 | 704 | 403 | 795 | 195 |
| **Brain Metabolite Level (mM)** | **Mean** | **SD** | **Mean** | **SD** | **Mean** | **SD** | **Mean** | **SD** |
| Left Caudate [d] tCho | 1.9 | 0.8 | 2.3 | 0.3 | 2.1 | 0.6 | 1.4 | 0.3 |
| Right Caudate tCho | 1.9 | 0.4 | 2.3 | 0.7 | 2.1 | 0.6 | 2.1 | 0.6 |
| Left Putamen tCho | 1.8 | 0.5 | 2.0 | 0.5 | 1.8 | 0.5 | 1.8 | 0.7 |
| Right Putamen tCho | 2.0 | 0.7 | 2.0 | 0.2 | 2.0 | 0.5 | 2.0 | 0.9 |
| Left Caudate [e] NAA | 7.5 | 2.5 | 9.8 | 1.6 | 8.7 | 2.3 | 6.5 | 1.6 |
| Right Caudate NAA | 9.4 | 2.2 | 9.4 | 2.0 | 9.4 | 2.0 | 8.1 | 1.8 |
| Left Putamen NAA | 9.8 | 2.3 | 11.3 | 1.2 | 10.6 | 1.9 | 9.8 | 2.9 |
| Right Putamen NAA | 11.1 | 2.6 | 11.1 | 1.3 | 11.1 | 1.9 | 9.2 | 0.7 |
| Left Caudate [f] tCr | 5.7 | 1.1 | 7.1 | 1.0 | 6.4 | 1.3 | 5.1 | 1.7 |
| Right Caudate tCr | 7.1 | 1.6 | 8.6 | 3.5 | 7.8 | 2.7 | 6.9 | 2.0 |
| Left Putamen tCr | 6.6 | 1.4 | 7.9 | 0.8 | 7.3 | 1.3 | 6.4 | 1.9 |
| Right Putamen tCr | 7.5 | 1.7 | 7.5 | 1.2 | 7.5 | 1.4 | 7.1 | 1.2 |

[a]3-Hydroxyanthranilic Acid;

[b]L-Kynurenine;

[c]L-Tryptophan;

[d]Total Choline;

[e]N-Acetylaspartate;

[f] Total Creatine;

[g] Standard Deviation